Mitigation of nonlinear distortion in hybrid Raman/phase-sensitive amplifier links

Mitigation of nonlinear distortion in hybrid Raman/phase-sensitive amplifier links

Henrik Eliasson,* Samuel L. I. Olsson, Magnus Karlsson and Peter A. Andrekson

Photonics Laboratory, Department of Microtechnology and Nanoscience, Chalmers University of Technology, SE-412 96, Gothenburg, Sweden

**henrik.eliasson@chalmers.se*

Abstract: Hybrid systems combining distributed Raman amplification and phase-sensitive amplifiers (PSAs) are investigated in numerical simulations. We focus on the mitigation of fiber nonlinearities and the impact of the span power map which is also important in systems employing optical phase conjugation or phase-conjugated twin waves. We simulate multi-span PSA links with and without distributed Raman amplification and show that by including distributed Raman amplification, the transmission distance increases more at optimum launch power than in the linear regime. For a 5-channel WDM QPSK PSA-amplified system, we observe a transmission reach increase by a factor of 8.1 by including ideal distributed Raman amplification.

OCIS codes: (060.0060) Fiber optics and optical communications; (060.4370) Nonlinear optics, fibers; (060.1660) Coherent communications.

References and links

1. C. M. Caves, "Quantum limits on noise in linear amplifiers," Phys. Rev. D **26**, 1817–1839 (1982).
2. Z. Tong, C. Lundström, P. A. Andrekson, C. J. McKinstrie, M. Karlsson, D. J. Blessing, E. Tipsuwannakul, B. J. Puttnam, H. Toda, and L. Grüner-Nielsen, "Towards ultrasensitive optical links enabled by low-noise phase-sensitive amplifiers," Nature Photon. **5**, 430–436 (2011).
3. S. L. I. Olsson, B. Corcoran, C. Lundström, M. Sjödin, M. Karlsson, and P. A. Andrekson, "Phase-sensitive amplified optical link operating in the nonlinear transmission regime," in Proc. European Conference on Optical Communications (ECOC) (2012), paper Th.2.F.1.
4. S. L. I. Olsson, B. Corcoran, C. Lundström, T. Eriksson, M. Karlsson, and P. A. Andrekson, "Phase-sensitive amplified transmission links for improved sensitivity and nonlinearity tolerance," J. Lightwave Technol. **33**, 710–721 (2015).
5. S. L. I. Olsson, C. Lundström, M. Karlsson, and P. A. Andrekson, "Long-haul (3465 km) transmission of a 10 GBd QPSK signal with low noise phase-sensitive in-line amplification," in Proc. European Conference on Optical Communications (ECOC) (2014), paper PD.2.2.
6. J. N. Kutz, C. V. Hile, W. L. Kath, R.-D. Li, and P. Kumar, "Pulse propagation in nonlinear optical fiber lines that employ phase-sensitive parametric amplifiers," J. Opt. Soc. Am. B **11**, 2112–2123 (1994).
7. X. Liu, A. R. Chraplyvy, P. J. Winzer, R. W. Tkach, and S. Chandrasekhar, "Phase-conjugated twin waves for communication beyond the Kerr nonlinearity limit," Nature Photon. **7**, 560–568 (2013).
8. X. Liu, S. Chandrasekhar, P. J. Winzer, R. W. Tkach, and A. R. Chraplyvy, "Fiber-nonlinearity-tolerant superchannel transmission via nonlinear noise squeezing and generalized phase-conjugated twin waves," J. Lightwave Technol. **32**, 766–775 (2014).
9. X. Liu, "Twin-wave-based optical transmission with enhanced linear and nonlinear performances," J. Lightwave Technol. **33**, 1037–1043 (2015).
10. H. Eliasson, S. L. I. Olsson, M. Karlsson, and P. A. Andrekson, "Comparison between coherent superposition in DSP and PSA for mitigation of nonlinearities in a single-span link," in Proc. European Conference on Optical Communications (ECOC) (2014), paper Mo.3.5.2.

#252368 Received 5 Nov 2015; revised 26 Dec 2015; accepted 26 Dec 2015; published 12 Jan 2016

11. H. Eliasson, P. Johannisson, M. Karlsson, and P. A. Andrekson, "Mitigation of nonlinearities using conjugate data repetition," Opt. Express **23**, 2392–2402 (2015).
12. A. Yariv, D. Fekete, and D. M. Pepper, "Compensation for channel dispersion by nonlinear optical phase conjugation," Opt. Lett. **4**, 52–54 (1979).
13. R. A. Fisher, B. R. Suydam, and D. Yevick, "Optical phase conjugation for time-domain undoing of dispersive self-phase-modulation effects," Opt. Lett. **8**, 611–613 (1983).
14. P. Kaewplung and K. Kikuchi, "Simultaneous cancellation of fiber loss, dispersion, and kerr effect in ultralong-haul optical fiber transmission by midway optical phase conjugation incorporated with distributed raman amplification," J. Lightwave Technol. **25**, 3035–3050 (2007).
15. K. Solis-Trapala, T. Inoue, and S. Namiki, "Signal power asymmetry tolerance of an optical phase conjugation-based nonlinear compensation system," in Proc. European Conference on Optical Communication (ECOC) (2014), paper We.2.5.4.
16. K. Solis-Trapala, M. Pelusi, H. N. Tan, T. Inoue, and S. Namiki, "Transmission optimized impairment mitigation by 12 stage phase conjugation of WDM 24×48 Gb/s DP-QPSK signals," in Proc. Optical Fiber Communications Conference and Exhibition (OFC) (2015), paper Th3C.2.
17. P. Rosa, G. Rizzelli, and J. D. Ania-Castañón, "Signal power symmetry optimization for optical phase conjugation using raman amplification," in Proc. Nonlinear Optics (NLO) (2015), paper NW4A.36.
18. A. D. Ellis, M. E. McCarthy, M. A. Z. Al-Khateeb, and S. Sygletos, "Capacity limits of systems employing multiple optical phase conjugators," Opt. Express **23**, 20381–20393 (2015).
19. X. Liu, H. Hu, S. Chandrasekhar, R. M. Jopson, A. H. Gnauck, M. Dinu, C. Xie, and P. J. Winzer, "Generation of 1.024-Tb/s Nyquist-WDM phase-conjugated twin vector waves by a polarization-insensitive optical parametric amplifier for fiber-nonlinearity-tolerant transmission," Opt. Express **22**, 6478–6485 (2014).
20. J.-C. Bouteiller, K. Brar, and C. Headley, "Quasi-constant signal power transmission," in Proc. European Conference on Optical Communications (ECOC) (2002), paper S3.04.
21. C. Headley and G. P. Agrawal, *Raman Amplification in Fiber Optical Communication Systems* (Elsevier Academic, 2005).
22. B. Corcoran, S. L. I. Olsson, C. Lundström, M. Karlsson, and P. A. Andrekson, "Mitigation of nonlinear impairments on QPSK data in phase-sensitive amplified links," in Proc. European Conference on Optical Communications (ECOC) (2013), paper We.3.A.1.
23. I. Sackey, R. Elschner, M. Nölle, T. Richter, L. Molle, C. Meuer, M. Jazayerifar, S. Warm, K. Petermann, and C. Schubert, "Characterization of a fiber-optical parametric amplifier in a 5 x 28-GBd 16-QAM DWDM system," in Proc. Optical Fiber Communication Conference (OFC) (2014), paper W3E.3.

1. Introduction

Coherent fiber-optic communication systems encode information on both the amplitude and phase of the optical field. These systems are typically used for digital communication over long distances, often thousands of kilometers. In such systems the maximum transmission distance is limited by amplified spontaneous emission (ASE) noise from in-line optical amplifiers and nonlinear signal distortion due to the Kerr effect.

Phase-sensitive amplifiers (PSAs) are capable of both low-noise optical amplification [1, 2], and mitigation of nonlinear fiber distortion [3, 4], leading to improved transmission reach over phase-insensitive amplifier (PIA)-amplified links [5]. In a single-channel link amplified by two-mode PSAs, two data-carrying waves at separate wavelengths are transmitted, the signal and a conjugate copy of the signal, commonly called idler. Each in-line PSA performs an all-optical coherent superposition of the signal and the idler, whereby correlated nonlinear distortions on signal and idler are mitigated [4]. Since the coherent superposition is performed all-optically in each PSA, the spans have to be dispersion compensated with limited residual dispersion. The use of inline PSAs in links operating in a nonlinear regime has also been investigated for soliton systems in [6], where it was shown that the stability of solitons could be improved with the use of inline PSAs.

A transmission scheme for nonlinearity mitigation that resembles PSA-amplified links is the phase-conjugated twin waves (PCTW) scheme [7–9]. In similarity to PSA-amplified links, two waves are transmitted, the signal and a conjugated copy of the signal, and the nonlinear distortion is mitigated by performing a coherent superposition of the two waves [7]. However, the waves are not superposed all-optically span-wise as in PSA-amplified links; instead they

#252368 Received 5 Nov 2015; revised 26 Dec 2015; accepted 26 Dec 2015; published 12 Jan 2016

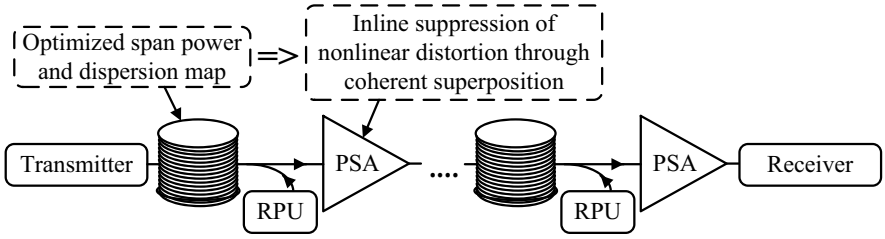

Fig. 1. A simplified schematic of the proposed system architecture that combines distributed Raman amplification with inline PSAs in order to mitigate nonlinear effects in an optimized manner. Raman pump unit (RPU), phase-sensitive amplifier (PSA).

are superposed in the receiver digital signal processing (DSP) after coherent detection of both waves separately. A comparison between the performance of coherent superposition in a PSA and in DSP was performed in [10]. Moreover, the waves can, e.g., be transmitted on orthogonal polarizations or in different time slots [11] instead of at different wavelengths.

Another scheme with similarities to PSA-amplified links is optical phase conjugation (OPC). Using this scheme, the signal is optically phase-conjugated at the center point of the link, whereby chromatic dispersion [12] and nonlinear distortion [13] introduced in the first half of the link is reversed in the second half. A drawback of the OPC scheme is that the link has to be physically altered by inserting an optical phase conjugator at the center point.

It has been shown that OPC [13] requires a symmetric power map in order to mitigate nonlinear distortions efficiently. In the case of PCTW, a symmetric or flat power map fulfills the assumptions made in the theoretical derivation in [7] meaning that there is good reason to believe that nonlinear distortion will be mitigated more efficiently with a symmetric power map in such systems, this has not been studied specifically however. It is not possible to achieve a symmetric power map in a system exclusively using lumped amplifiers, such as PSA-amplified links. However, by introducing Raman amplification, a higher degree of symmetry of the span power map around the center point can be obtained.

Raman amplification has previously been investigated in both OPC links [14–18] and in PCTW links [19]. However, in PCTW links it is not known how much the nonlinearity mitigation is improved by having a higher degree of power map symmetry, e.g., from Raman amplification, in either single- or multi-span links. Moreover, it is not known how much a power map with a higher degree of symmetry will improve the nonlinearity mitigation in multi-span links employing span-wise coherent superposition of the signal and conjugated copy, e.g, using PSAs.

In this paper we propose to combine distributed Raman amplification with inline PSAs. A simplified schematic of such a system is shown in Fig. 1. We investigate numerically, the impact of distributed Raman amplification on the performance, in a nonlinear regime, of fiber-optic communication systems that perform coherent superposition using PSAs. First, a single-span system is studied to determine in which cases it is beneficial to make use of Raman amplification in such systems. Then we investigate a multi-span system that performs the coherent superposition span-wise using PSAs. The role of the span power map in these systems is discussed and we show that there are significant performance gains possible for a multi-span system in the nonlinear regime by increasing the degree of symmetry of the span power map with the use of distributed Raman amplification. An important feature of a PSA is that the quantum limited noise figure is lower than for a PIA, e.g. an erbium-doped fiber amplifier (EDFA), 0 dB compared to 3 dB [2]. However, this distinguishing feature becomes of less relevance in a

#252368 Received 5 Nov 2015; revised 26 Dec 2015; accepted 26 Dec 2015; published 12 Jan 2016

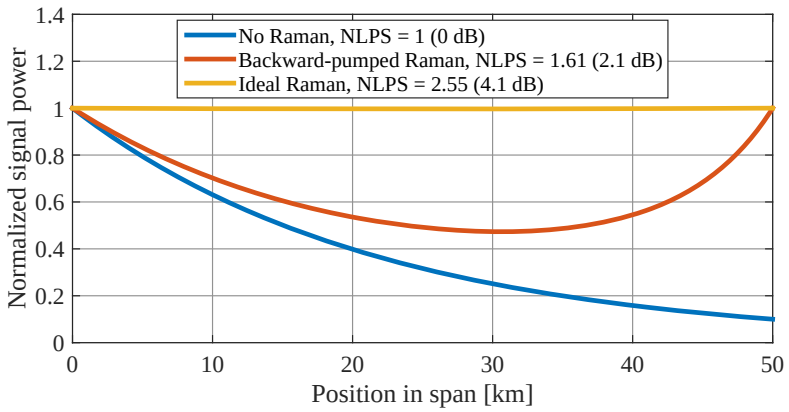

Fig. 2. The span power maps of the three investigated amplifier configurations. The nonlinear phase shift (NLPS) specified in the legend has been normalized to that of a span without distributed Raman amplification.

Raman-amplified PSA link since the noise power generated by the distributed Raman amplification always will be higher than the noise power generated by the PSAs. This means that for a Raman-PSA hybrid system, the low noise requirements on the PSA could be relaxed, possibly leading to less complex PSA implementations.

The paper is organized as follows: In Section 2, we present a background on PSA-amplified systems and the use of distributed Raman amplification in such systems. Following that, a description of the computer simulations is presented in Section 3. The results from the computer simulations are presented in Section 4, followed by a discussion of the results in Section 5.

2. Distributed Raman amplification in PSA systems

The importance of the dispersion map in systems that transmit a conjugated copy alongside the signal followed by coherent superposition was first highlighted by Liu et al. [7]. In that paper it was shown, to first order, that the nonlinear distortion is cancelled in the coherent superposition operation under certain assumptions regarding the dispersion map and logarithmic signal power evolution. If a symmetric power map is assumed, the assumption regarding the logarithmic signal power evolution will hold. Even though the system investigated in that paper is different compared to a multi-span PSA system performing coherent superposition periodically in each span, the theory applies with minor modification to a single-span system or, in a multi-span system, to each of the spans individually. Thus it is reasonable to assume that in order for a multi-span PSA system to perform optimally in the nonlinear regime, efforts should be made to achieve a span power map with a high degree of symmetry around the center point of the span.

The simplest way of using distributed Raman amplification in order to increase the span power map degree of symmetry is to use backward-pumped Raman amplification. Assuming that the span loss is fully compensated by the Raman gain, the span power map will depend on three system parameters, the span length and the losses at the Raman pump and signal wavelengths. For shorter spans or with lower loss at the Raman pump wavelength, it is possible to achieve a higher degree of symmetry of the span power map. Other ways of further manipulating the span power map are, e.g., by the use of a combination of forward- and backward-pumped Raman amplification or by using higher-order Raman pumps. An investigation of such amplifier configurations is however outside the scope of this paper. When discussing symmetric power maps in Raman-amplified systems, we note that this is not unrealistic. In [20], an

#252368 Received 5 Nov 2015; revised 26 Dec 2015; accepted 26 Dec 2015; published 12 Jan 2016

Table 1. Fiber parameters used in simulations.

parameter	value	unit
L_{fiber}	50	[km]
α_{signal}	0.2	[dB/km]
$\alpha_{\text{pump,backward}}$	0.25	[dB/km]
$\alpha_{\text{pump,ideal}}$	0.001	[dB/km]
g_{R}	0.3	[1/(W·km)]
D	17	[ps/(nm·km)]
γ	1.3	[1/(W·km)]

almost perfectly flat power map with power variations of only ± 0.4 dB over a 80 km span was achieved with the use of bi-directional second-order Raman pumps.

We compare three different amplifier configurations. First, only PSA amplification, second, PSA together with backward-pumped Raman amplification and third, PSA together with ideal Raman amplification with a flat power map. The flat power map is achieved by setting the attenuation at the Raman pump wavelength $\alpha_{\text{pump,ideal}} = 0.001$ [dB/km] instead of $\alpha_{\text{pump,backward}} = 0.25$ [dB/km]. The degree of symmetry of the span power map for a backward-pumped Raman system is higher with shorter spans, because of this we choose to simulate systems with a relatively short span length of 50 km. The span power maps of the three systems are shown in Fig. 2.

When comparing the resilience against nonlinear effects of PSA systems with and without Raman amplification, the strength of the nonlinearity is quantified both in terms of the launch power and the accumulated nonlinear phase shift (NLPS). Since the Raman-amplified systems have a distributed gain, the accumulated NLPS at a given launch power will be higher. The span power maps $G(z)$ are calculated as [21, Eq. 2.1.14]

$$G(z) = \frac{P_{\text{signal}}(z)}{P_{\text{signal}}(0)} = \exp\left(g_{\text{R}} P_{\text{pump}} \int_0^z \exp\left(-\alpha_{\text{pump}}(L_{\text{fiber}} - z')\right) dz' - \alpha_{\text{signal}} z\right), \tag{1}$$

where g_{R} is the Raman gain coefficient and we assume that we are operating in an undepleted pump regime. The corresponding NLPS is calculated as

$$\Phi_{\text{NL}}(z) = \int_0^z \gamma P_{\text{signal}}(z') dz'. \tag{2}$$

Compared to the system without Raman amplification at any given launch power, the NLPS of the backward-pumped Raman system is increased by a factor of 1.61 (2.1 dB) and with the flat ideal Raman power map, it is increased by a factor of 2.55 (4.1 dB). These values are valid with the fiber span parameters shown in Table 1.

3. Computer simulations

Computer simulations were carried out in order to optimize the dispersion map for single-span PSA links with and without backward-pumped Raman amplification and after that, to estimate the performance of single-span and multi-span links with the found dispersion maps. A schematic of the simulated system is shown in Fig. 3. A non-return-to-zero quadrature phase-shift keying (QPSK) or 16-ary quadrature amplitude modulation (16QAM) signal, as a single-channel or with wavelength-division multiplexing (WDM), is generated together with a conjugated copy in the transmitter. A phase-locked conjugated copy can be generated e.g. using a phase-insensitive parametric amplifier, then called copier, or by modulating different lines of a

#252368 Received 5 Nov 2015; revised 26 Dec 2015; accepted 26 Dec 2015; published 12 Jan 2016

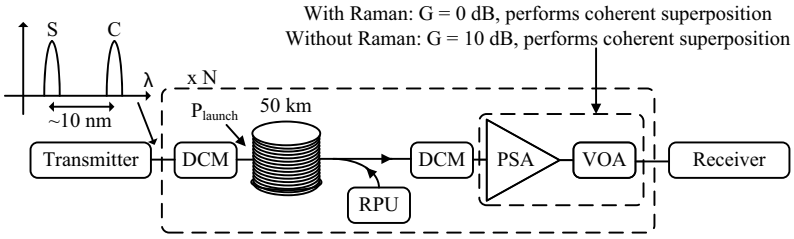

Fig. 3. Schematic of the simulated system. Dispersion compensating module (DCM), Raman pump unit (RPU), variable optical attenuator (VOA), signal (S), conjugate copy (C).

coherent comb. The signal and conjugate are then dispersion pre-compensated in the first dispersion compensating module (DCM) before being launched into the transmission fiber. The DCMs are assumed to have negligible nonlinearities, this is reasonable assuming that we are using fiber Bragg grating-based DCMs. The propagation in the fiber is modeled using the split-step Fourier method, taking the power map due to backward-pumped Raman amplification into account according to Eq. (1). The signal and conjugate waves are propagated by separate nonlinear Schrödinger equation (NLSE) solvers, not taking higher order dispersion or polarization mode dispersion (PMD) into account. Separate NLSE solvers is a reasonable approximation since it is assumed that the signals are separated by approximately 10 nm. This was also confirmed by using one solver that propagated the whole spectrum of the signal and conjugated copy separated by 10 nm which gave similar results. After each fiber span is a Raman pump unit (RPU) pumping in the backward direction and the ASE noise generated by the Raman amplification is added in a lumped manner at the end of each span. In all cases with Raman amplification, the Raman pump power is chosen so that the span net gain is 0 dB. The power spectral density of the ASE noise added after each span was calculated as [21, Eq. 2.2.5]

$$S_{\mathrm{ASE}} = n_{\mathrm{sp}} h \nu_0 g_{\mathrm{R}} \int_0^{L_{\mathrm{fiber}}} \frac{P_{\mathrm{pump}} \exp\left(-\alpha_{\mathrm{pump}}(L_{\mathrm{fiber}} - z)\right)}{G(z)} dz, \tag{3}$$

where n_{sp} is the spontaneous-scattering factor, ν_0 is the optical frequency of the amplified signal and h is Plancks constant. Before each PSA, the signal is dispersion post-compensated by a DCM. The PSA is simulated as the concatenation of a PIA with a 0 dB noise figure followed by coherent superposition of the signal and conjugate fields according to

$$\begin{pmatrix} E_{\mathrm{signal,out}} \\ E^*_{\mathrm{conjugate,out}} \end{pmatrix} = \frac{1}{2} \begin{pmatrix} 1 & 1 \\ 1 & 1 \end{pmatrix} \begin{pmatrix} E_{\mathrm{signal,in}} \\ E^*_{\mathrm{conjugate,in}} \end{pmatrix}. \tag{4}$$

This is approximately achieveable by a high-gain PSA followed by an attenuator. The noise generated in this process can be neglected relative to the Raman ASE noise. The input signal and conjugate fields were phase aligned with the criterion that the power of the output fields should be maximized. We note that the purpose behind using PSAs in our proposed scheme is not low-noise amplification but for suppression of nonlinear distortion. In the cases where Raman amplification is used in combination with PSAs, the PSA should not supply any gain and because of this, a variable optical attenuator (VOA) is placed after the PSA in order to get the correct launch power into the following span. In the case of amplification by EDFA only, the PSA is replaced by an EDFA with a 3 dB noise figure. In the cases with only Raman amplification, the PSA and VOA is removed. The parameters of the optical fiber are shown in Table 1.

#252368 Received 5 Nov 2015; revised 26 Dec 2015; accepted 26 Dec 2015; published 12 Jan 2016

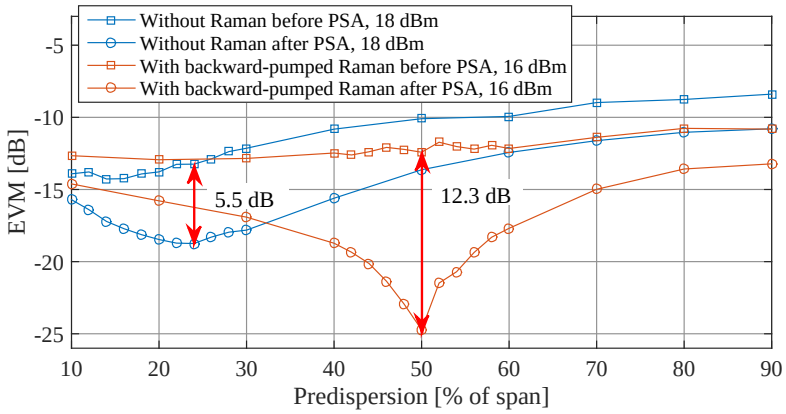

Fig. 4. EVM before and after the PSA as a function of dispersion pre-compensation with and without backward-pumped Raman amplification in a single-span system. Launch powers are specified in the legend.

For single-span simulations, a waveform length of 2^{17} symbols was used. In order to reduce simulation run times, shorter waveforms with length 2^{10} were used for all multi-span simulations where error vector magnitude (EVM) was used to estimate signal quality. In all simulations, the transmitted data was random. The waveforms were sampled with 32 samples per symbol. The step sizes of the NLSE solver was 5 m for the single-span simulations and 50 m for the multi-span simulations.

4. Results

The results are presented in three subsections. First, results from the single-span dispersion map optimization and optical signal-to-noise ratio (OSNR) penalty simulations, second, the results from multi-span single-channel simulations and third, the results from multi-span WDM simulations.

4.1. Single-span results

In order to optimize the dispersion map for a single-span link with and without Raman amplification, the amount of dispersion pre-compensation was varied before launching the signal and conjugate into the span. This has previously also been investigated for a single-span link without Raman amplification at low symbol rate (10 GBaud) in [22]. The launch power was set to 16 dBm for the system with backward-pumped Raman amplification and to 18 dBm for the system without Raman amplification. The launch powers are specified as the total power of the signal and the conjugate copy. These launch powers were chosen so that the accumulated nonlinear phase shift is approximately the same for both systems. After the span, the EVM was calculated before and after the PSA. The signal was 112 GBaud QPSK. The results from these simulations are shown in Fig. 4. For these simulations there was no addition of AWGN meaning that the increase in EVM is caused only by nonlinear effects. The optimum was chosen as the point with the lowest EVM after coherent superposition. It is seen that the system without Raman amplification has an optimum at 24 % pre-compensation (12 km) while the system with Raman amplification has an optimum at 50 % (25 km). From the theory presented in [7] we would expect an optimum close to 50 % for the system with Raman amplification since the span power map has a high degree of symmetry. The EVM improvement due

#252368 Received 5 Nov 2015; revised 26 Dec 2015; accepted 26 Dec 2015; published 12 Jan 2016

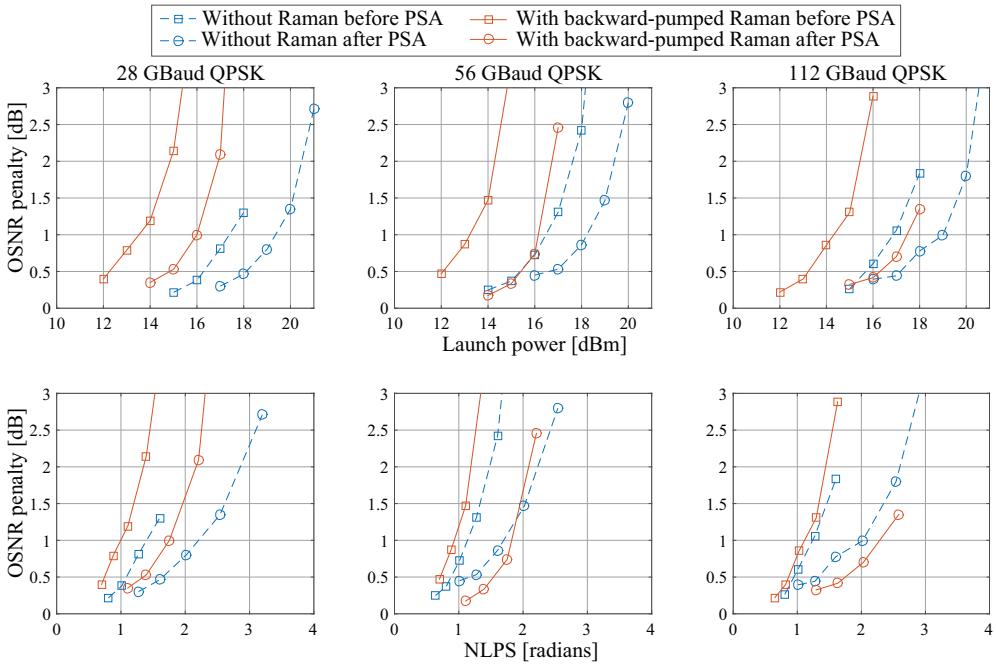

Fig. 5. The OSNR penalty at BER = 10^{-3} as a function of launch power (top row) and NLPS (bottom row) in a single-span PSA link with and without Raman amplification for 28, 56 and 112 GBaud QPSK, respectively.

to coherent superposition is larger in the Raman-amplified system (12.3 dB) compared to the system without Raman amplification (5.5 dB). Also we see that the absolute value of the EVM is lower in the Raman-amplified system (−24.7 dB) compared to the system without Raman amplification (−18.7 dB). Already here we see an indication that the PSA system with Raman amplification mitigates nonlinear effects more efficiently at high symbol rates, even for the least complex implementation of distributed Raman amplification with a single backward pump.

Following this, simulations were performed to quantify the effect of backward-pumped Raman amplification at three different symbol rates, 28, 56 and 112 GBaud. For these simulations, the signal was propagated over a single span and then noise loaded before the receiver where the BER was counted. The dispersion maps were chosen according to the optima found in the dispersion map optimization (24 % without Raman amplification and 50 % with Raman amplification). The results from these simulations are shown in Fig. 5. The top row shows the OSNR penalty at BER = 10^{-3} as a function of launch power and the bottom row shows the OSNR penalty as a function of the associated accumulated NLPS. We see in these figures that the resilience against nonlinear effects after coherent superposition of the Raman-amplified system improves compared to the system without Raman amplification as we move to higher symbol rates. At 28 GBaud, the system without Raman amplification performs better than the system with Raman amplification at all launch powers and NLPS. The reason for this is that the nonlinear distortion at low symbol rates and a low amount of dispersion pre-compensation is approximately a self-phase modulation (SPM) rotation of the constellation and QPSK is resilient against pure SPM rotations. At 112 GBaud, the Raman-amplified system has a lower OSNR penalty after coherent superposition at all NLPS indicating that the mitigation of nonlinear effects is more efficient with Raman amplification at high symbol rates. We draw the

#252368 Received 5 Nov 2015; revised 26 Dec 2015; accepted 26 Dec 2015; published 12 Jan 2016

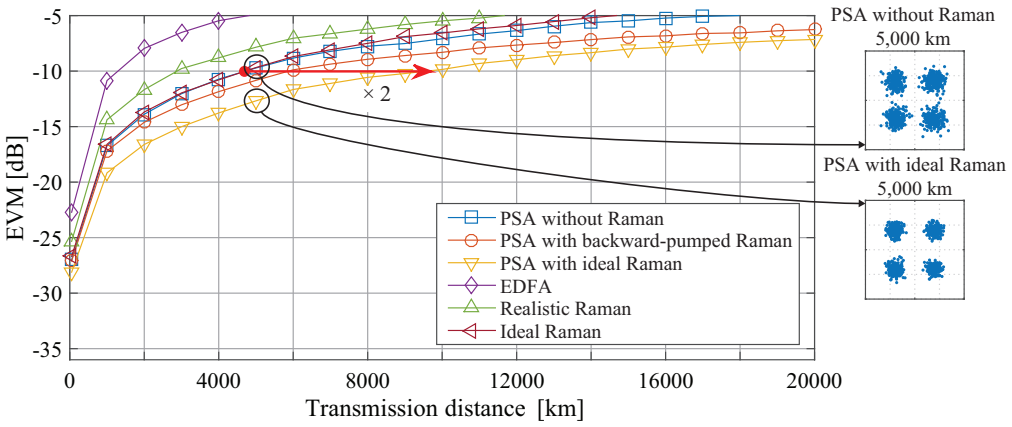

(a)

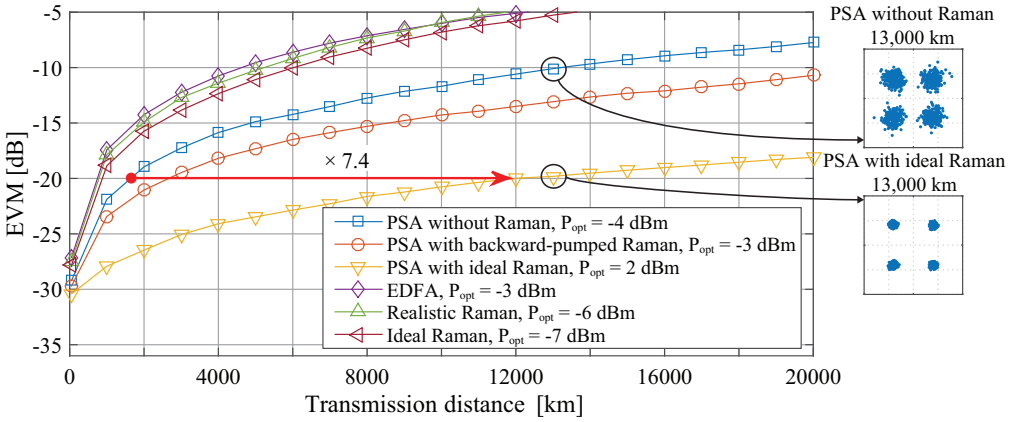

(b)

Fig. 6. EVM as a function of transmission distance of 112 GBaud single-channel QPSK systems in (a) quasi-linear regime with -10 dBm launch power and (b) nonlinear regime at optimum launch powers, as indicated for each system in the legend. The increase in transmission distance at the chosen EVM levels by addition of ideal Raman amplification in a PSA system is marked in the figure. Shown in the figure are also example constellation diagrams for the PSA system without Raman amplification and the PSA system with ideal Raman amplification.

conclusion that in order to observe significant improvements from Raman amplification in the nonlinear domain, we should operate at high symbol rates, or alternatively with many WDM channels as will be shown in Section 4.3.

4.2. Single-channel multi-span results

For the multi-span simulations the optimum dispersion maps found in the single-span simulations were used and the symbol rate was set to 112 GBaud. The performance of the multi-span systems was quantified by the EVM. The EVM as a function of the transmission distance for the different amplifier configurations is shown in Fig. 6. There are also example constellation diagrams in the figure, comparing the constellation diagrams of the PSA system without Raman amplification at EVM ≈ -10 dB to the constellations of the PSA system with ideal Raman

#252368 Received 5 Nov 2015; revised 26 Dec 2015; accepted 26 Dec 2015; published 12 Jan 2016

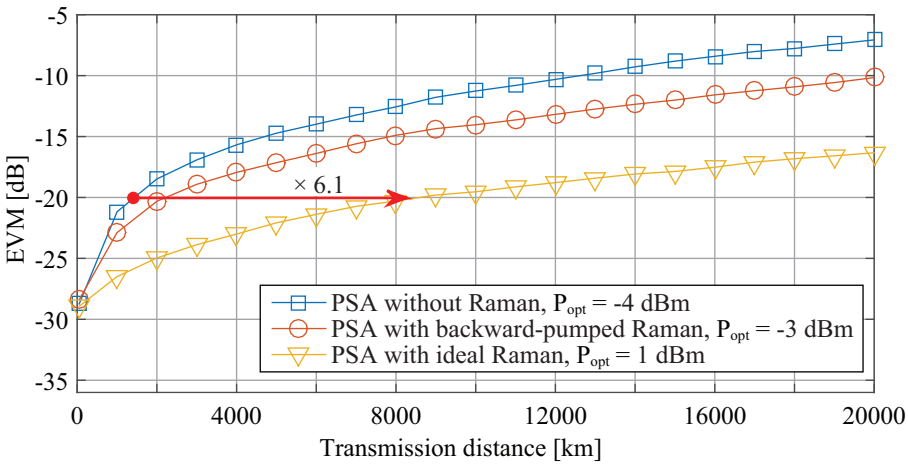

Fig. 7. EVM as a function of transmission distance of single-channel 112 GBaud 16QAM systems at the optimum launch power.

amplification at the same transmission distance. An EVM of -10 dB was chosen since it corresponds approximately to a BER $= 10^{-3}$ for QPSK. These constellations illustrate the difference in the observed EVM improvement due to ideal Raman amplification in linear domain and at optimum launch powers. In order to evaluate whether a multi-span PSA system with Raman amplification mitigates nonlinear effects more efficiently we compare the transmission distances of PSA systems with and without distributed Raman amplification in a linear regime (-10 dBm launch power) and in the nonlinear regime with optimized launch powers. The launch powers were optimized in order to minimize the EVM at long transmission distances.

In the low-power regime (-10 dBm launch power), the transmission distance at EVM $=$ -10 dB increases from 4,700 km (PSA without Raman) to 5,850 km (PSA with backward-pumped Raman) and to 9,550 km (PSA with ideal Raman amplification). For the system with backward-pumped Raman this corresponds to an increase in the transmission distance by a factor of approximately 1.2 and for the ideally Raman amplified system by a factor of 2.0. Since the EVM of the ideally Raman-amplified PSA system at optimum launch power doesn't reach an EVM higher than -18 dB even at long transmission distances, we have to make the comparison at a lower EVM. If we do the same comparison at optimum launch powers and an EVM of -20 dB, the transmission distance increases from 1,600 km (PSA without Raman, -4 dBm) to 2,650 km (PSA with backward-pumped Raman, -3 dBm) and to 11,900 km (PSA with ideal Raman amplification, 2 dBm). This corresponds to increases in transmission distance by factors of 1.7 and 7.4. We see that at optimum launch powers the increases in transmission distance are significantly larger compared to the linear domain, both with backward-pumped Raman amplification and especially with ideal Raman amplification. Also worth noting here is that the optimum launch powers are increased in the systems employing Raman amplification, from -4 dBm without Raman amplification to -3 dBm with backward-pumped Raman and 2 dBm with ideal Raman amplification. The optimum launch powers increase even though the nonlinear effects are stronger at the same launch power in the Raman-amplified systems due to the flatter power maps. In terms of NLPS at optimum launch power, this corresponds to increases of 3.1 dB (PSA with backward-pumped Raman amplification) and 10.1 dB (PSA with ideal Raman amplification). The NLPS of the signal in the ideally Raman-amplified PSA link at 20,000 km is 21 radians, still the system is operating at an EVM of approximately -18 dB. This is possible only thanks to the periodic PSA nonlinearity suppression.

#252368 Received 5 Nov 2015; revised 26 Dec 2015; accepted 26 Dec 2015; published 12 Jan 2016

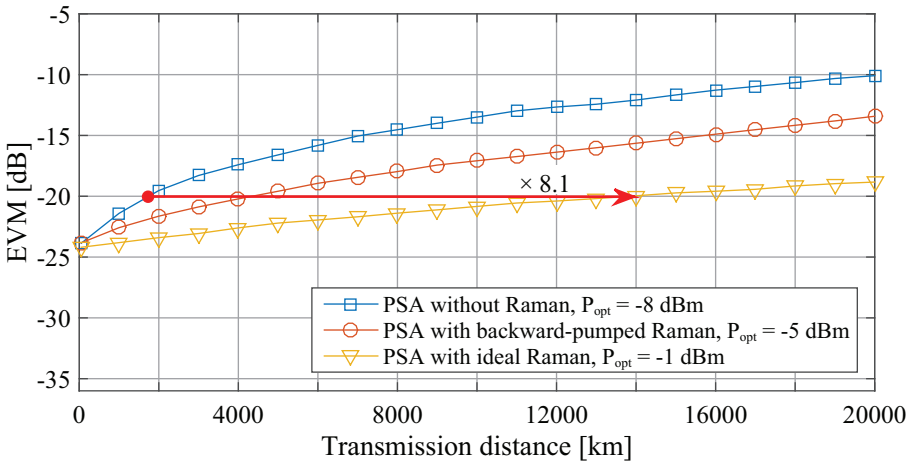

Fig. 8. EVM as a function of transmission distance for 5-channel WDM 28 GBaud QPSK systems at optimum launch powers.

Simulations were also performed to investigate if a PSA link transmitting 16QAM would benefit to the same extent from Raman amplification. The symbol rate was kept at 112 GBaud and the same dispersion maps found to be optimal in the single-span case with QPSK data were used. The results from these simulations are shown in Fig. 7 where a PSA system without Raman amplification is compared to systems with backward-pumped and ideal Raman amplification. If we compare the transmission distance at an EVM of −20 dB in the same way as for the QPSK systems, the transmission distance increases from 1,400 km (PSA without Raman, −4 dBm) to 2,200 km (PSA with backward-pumped Raman, −3 dBm) and to 8,550 km (PSA with ideal Raman amplification, 1 dBm), which corresponds to factors of 1.6 and 6.1, respectively. The increases in transmission distance due to the addition of Raman amplification is smaller for 16QAM systems compared to QPSK systems but still significant. We also note that the ideally Raman amplified PSA system transmitting 16QAM has a 1 dB lower optimum launch power (1 dBm) compared to the same system transmitting QPSK (2 dBm).

4.3. WDM multi-span results

Simulations were also performed in order to evaluate if the resilience to nonlinear effects of a WDM PSA system can be improved by the addition of Raman amplification. For these simulations, instead of a single-channel 112 GBaud signal, we used a 5-channel WDM 28 GBaud QPSK signal. The channel spacing was 50 GHz. For this case it is important to note that the conjugated copy is generated by conjugation of the waveform of the entire WDM grid and not by conjugation of the channels individually. The EVM of the center channel as a function of transmission distance for the WDM systems is shown in Fig. 8. If comparing the WDM results to the single-channel results, we note that the channel symbol rate is lower, 28 GBaud compared to 112 GBaud, which is why the EVM values in absolute terms are lower compared to those of the single-channel systems. If we do the same comparison as in the previous cases and compare the transmission distances at an EVM of −20 dB, we see that the transmission distance increases from 1,700 km (PSA without Raman, −8 dBm) to 4,300 km (PSA with backward-pumped Raman, −5 dBm) and to 13,800 km (PSA with ideal Raman, −1 dBm). This corresponds to increases in transmission distances by factors of 2.5 and 8.1, again much larger increases than those seen in the linear regime where the transmission distance was increase by factors of 1.2 and 2. Since the conjugation in the transmitter is performed on the whole WDM spectrum, one

#252368 Received 5 Nov 2015; revised 26 Dec 2015; accepted 26 Dec 2015; published 12 Jan 2016

would expect that inter-channel nonlinear effects are mitigated as well which is confirmed by the simulations.

5. Discussion and conclusion

We have numerically studied the impact of the span power map on single- and multi-span PSA systems operating in the nonlinear regime. In order to achieve a higher degree of symmetry of the span power map we have employed distributed Raman amplification in two ways, first, with backward-pumped Raman amplification and second, with ideal distributed Raman amplification.

For the single-span case we have optimized the dispersion maps and investigated the effect of the symbol rate. It was found that the impact of the span power map became larger at high symbol rates. At 112 GBaud, the OSNR penalty of the single-span PSA system with Raman amplification was lower than that of the PSA system without Raman amplification at all NLPS. In the following argument, we focus on PSA systems without Raman amplification, i.e. an exponentially decaying span power map. In order to understand the impact of the symbol rate we compare the effective length $L_{\text{eff}} = (1-\exp(-\alpha L))/\alpha$ to the dispersive length L_{D} at the three studied symbol rates. Assuming $L_{\text{D}} \approx T_{\text{S}}^2/|\beta_2|$, where T_{S} is the symbol duration, we get $L_{\text{D,28G}} \approx 59$ km, $L_{\text{D,56G}} \approx 15$ km and $L_{\text{D,112G}} \approx 4$ km. At 28 GBaud, the dispersive length is longer than the effective length, 59 km compared to 21 km, meaning that in a perturbation analysis, the nonlinear distortion generated in the beginning of the span is similar to the distortion generated at the end of the effective length, reducing the impact of the span power map. At 112 GBaud, the dispersive length is shorter than the effective length, 4 km compared to 21 km. In this case, the nonlinear distortion generated in the beginning of the span is different from the nonlinear distortion generated at the end of the effective length, due to the strong dispersive effects at high symbol rates. With this in mind, it is reasonable to assume that the optimization of the span power map becomes more important at higher symbol rates, which is also seen in the single-span simulation results, or with many WDM channels. This conclusion holds also for a multi-span PSA system which can be seen as a concatenation of many single-span systems.

In a multi-span system we have shown that distributed Raman amplification increases the resilience to nonlinear effects of multi-span PSA links leading to an increase in transmission distance at optimum launch power for a single-channel 112 GBaud QPSK system with ideal Raman amplification by a factor of 7.4. For a 5-channel WDM 28 GBaud QPSK system the transmission distance was increased by a factor of 8.1 by the addition of ideal Raman amplification, showing that the concept can mitigate also inter-channel nonlinear effects. This should however not be interpreted as if the ideally Raman-amplified system mitigates nonlinear distortion more efficiently in a WDM scenario, rather that the system without Raman amplification is more degraded by inter-channel nonlinear effects. The increases in transmission distance at optimum launch powers are much larger compared to the increases observed in linear regime where the transmission distance is increase by a factor of 2 with the addition of ideal distributed Raman amplification. We also investigated a 112 Gbaud 16QAM system which showed an increase in the transmission distance by a factor of 6.4 by the addition of ideal Raman amplification. The observed NLPS for the QPSK PSA system with ideal Raman amplification at 20,000 km transmission distance and optimum launch power (2 dBm) is remarkably high at 21 radians, this is possible only thanks to the suppression of nonlinear distortion in the inline PSAs.

Even though the gains due to ideal Raman amplification in the computer simulations are substantial, several challenges remain regarding the practical implementability of a hybrid Raman-PSA system. One important issue is the effect of PMD in a multi-span hybrid Raman-PSA system with wide transmission bandwidth but investigating this is outside the scope of this pa-

#252368 Received 5 Nov 2015; revised 26 Dec 2015; accepted 26 Dec 2015; published 12 Jan 2016

per. Building a high-gain parametric amplifier that can handle high input powers above 0 dBm might also be difficult due to crosstalk within the amplifier [23]. Another important challenge is to achieve a span power map which is close to ideal distributed Raman amplification with good noise properties using bi-directional higher-order Raman pump schemes even though this is a previously well investigated subject. The backward-pumped system did not show as large increase in transmission distance compared to the PSA system without Raman amplification when going from linear domain (factor of 1.2) to optimum launch power (factor of 1.7) as the ideally Raman-amplified system.

We conclude that the span power map can be an important factor in the performance optimization of multi-span transmission systems which perform span-wise coherent superposition using PSAs.

Acknowledgments

This work is supported by the European Research Council under grant agreement ERC-2011-AdG - 291618 PSOPA and by the Knut and Alice Wallenberg Foundation.

#252368 Received 5 Nov 2015; revised 26 Dec 2015; accepted 26 Dec 2015; published 12 Jan 2016